Cumhuriyet Sci. J., 46(1) (2025) 172-178
DOI: https://doi.org/10.17776/csj.1632158

Cumhuriyet Science Journal

| csj.cumhuriyet.edu.tr | Founded: 2002 ISSN: 2587-2680 e-ISSN: 2587-246X Publisher: Sivas Cumhuriyet University

Design and Fabrication of Single Transverse Mode Passive Large-Pitch Fibers

Bülend Ortaç [1,a,*]

[1] *UNAM-National Nanotechnology Research Center and Institute of Materials Science and Nanotechnology, Bilkent University, Ankara 06800, Türkiye*
**Corresponding author*

Research Article

History
Received: 03/02/2025
Accepted: 21/03/2025

ABSTRACT

The fabrication processes of single transverse mode passive large-pitch optical fiber (LPF) have been proposed and investigated. The LPF design, combined with the fundamental mode operating principle of delocalizing higher-order modes, has led to impressive performance. In this study, two LPF preform designs were proposed based on the stacking of one type of inner glass tube, two (design of LPF1) or three (design of LPF2) different filler rods, and a core rod placed within an outer tube. The first passive LPF1 is fabricated from a single-step preform drawing process. This fiber exhibits single transverse mode propagation, featuring a core size of 45.5 µm and a normalized hole diameter of 0.454. For the first time, a single transverse mode of light propagation from an LPF with an elliptical-like hole shape was achieved. The second LPF2 design has been proposed and fabricated by using a two-step preform drawing process. Successful production of an LPF with a circular hole shape has been obtained and exhibits single transverse mode propagation, featuring a core size of 42.8 µm and a normalized hole diameter of 0.322. Furthermore, numerical analysis was also performed to study mode propagation for the LPF.

Keywords: Photonic crystal fiber, Large-pitch fiber, Large-mode-area, Single transverse mode

[a] *ortac@unam.bilkent.edu.tr* *https://orcid.org/0000-0002-1104-7459*

Introduction

Fiber laser oscillator and amplifier systems comprise several critical components, including semiconductor diode lasers, pump combiners, fiber Bragg gratings, saturable absorbers, stretchers, compressors, and active fibers [1-4]. Among these, active fiber is an essential component for generating and amplifying the laser signal. Step-index optical fiber can be effectively utilized for light amplification in fiber laser systems. In such applications, the core of the fiber is doped with rare-earth elements, such as ytterbium or erbium, which serve as the amplifying medium. Power scaling in fiber laser systems initiates non-linear interactions that arise from these effects, including Self-phase modulation (SPM) and Stimulated Raman Scattering (SRS) [1-4]. To control these effects, large-mode-area step-index optical fibers have been proposed [5, 6]. This type of fiber provides a larger core diameter, which helps to reduce nonlinear effects and allows for higher power amplification. The design of large-mode-area step-index fibers enhances the efficiency of the laser system by enabling better control over the beam quality by reducing the core numerical aperture and minimizing signal distortion. However, this approach also creates a platform for the interaction between the fundamental mode and higher-order modes (HOMs) at certain power levels, which can noticeably reduce the quality of the laser beam, called Transverse Mode Instability (TMI) [7]. To increase the power scaling attainable with fiber lasers, one effective strategy is to enlarge the single-transverse mode areas. This approach allows for better handling of higher energy densities, leading to improved performance and efficiency in the amplification process. By optimizing the new designs of the fiber and its core structures, it becomes possible to achieve higher output powers while maintaining beam quality. Key innovations include chirally-coupled core fibers [8], which improve mode coupling efficiency, and distributed mode filtering rod-type fibers [9] that help suppress unwanted modes. Other notable designs are leakage channel fibers [10], which minimize modal dispersion, and multitrench fibers [11], which maximize mode-field area without compromising single-mode characteristics. Additionally, photonic bandgap fibers [12] and Bragg fibers [13] have been developed to leverage optical bandgap phenomena for better light confinement. Lastly, LPFs offer significant advantages in achieving a large-mode area while ensuring effective single-mode operation [14, 15]. These fibers present transverse mode discrimination through a combination of differential propagation losses on the fundamental mode compared to HOMs and preferential excitation of the fundamental mode, which currently shows records of mode area, power, and energy scaling performances in fiber laser systems [16-19]. In the literature, there is no detailed guidance for single transverse mode LPF fabrication. In this study, the manufacturing processes of single transverse mode passive LPF with different designs are reported. Detailed designs consist of stacking and drawing the LPF preforms from a single- or two-step preform drawing process. LPFs with circular or elliptical-like hole-shaped structures have been produced. Single transverse mode propagations have been confirmed from the LPF featuring a core size of 45.5 µm and a normalized hole

diameter of 0.454 from elliptical-like hole-shaped and the LPF featuring a core size of 42.8 µm and a normalized hole diameter of 0.322 from circular hole-shaped, respectively. In addition, numerical analysis was also investigated to study single-mode propagation for the fiber.

Design of Single Transverse Mode Passive Large-Pitch Fiber

The representative structure of the LPF cross-section is shown in Figure 1. All the LPF designs considered in this paper have hexagonal photonic crystal fiber concepts without an air-cladding ring. The fiber core is formed by one missing hole. The fiber core size can be determined as a region from the corner of holes with a diameter of D. This fiber core is then surrounded by two hexagonal rings of air holes with equidistant air hole distances. In LPF geometry, the pitch Λ is called the hole-to-hole distance, and d is called the diameter of the hole. The normalized hole-diameter d/Λ plays a key role in the fiber guidance properties. The single-mode criteria in the solid-core PCFs can be associated with d/Λ values below 0.4 [20]. To eliminate the index-depressions issue on the light guidance in the core compared to the cladding region, the refractive index of the cladding region (ncladding) and core region (ncore) are chosen at the same refractive index level shown in Figure 1.

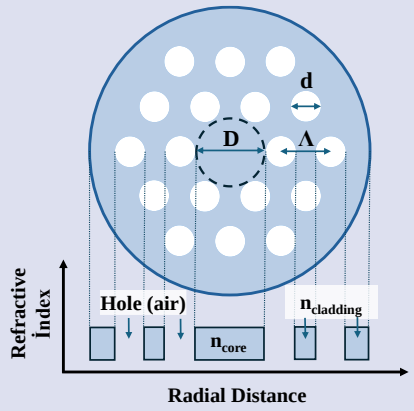

Figure 1. Schematic diagram of an LPF cross-section. The fiber structure consists of a hexagonal two-ring structure with equidistant air holes separated by a pitch Λ and a diameter d with one missing hole as a core (diameter D).

Fabrication of LPF with Single-step Drawing Processing

Figure 2a shows details of the first LPF1 design. It consists of 18 identical (outer diameter and thickness) inner tubes arranged with two hexagonal structures in an outer tube. The inner tube size parameters (inner and outer diameters) determine the LPF fiber pitch Λ and diameter(d) of the hole. The size of the inner tubes has been carefully designed to optimize the d/Λ parameter during the drawing process. A rod with the same diameter as the outer diameter of the inner tube is then placed in the center of the design. To fix this structure into an outer tube, 2 different-sized filler rods (12 pieces each) have been added to this structure, as shown in Figure 2a. An image of this LPF1 preform design without an outer tube has been presented in Figure 2b. The design of the final PCF depends on the preform drawing conditions. The size of the PCF preform is often adjusted to be in a cm scale. The PCF preform can be drawn in one step in which PCFs can be directly obtained upon the fiber drawing. On the other hand, when the PCF is drawn in two step conditions, then a PCF preform with a relatively smaller size called PCF cane is obtained in the order of mm scale. The design of the PCF preform determines what the final PCF structural units are, such as the number of air holes and the size of the PCF core will become. However, the light guiding properties will depend on the drawing conditions and the final fabricated design of the PCFs.

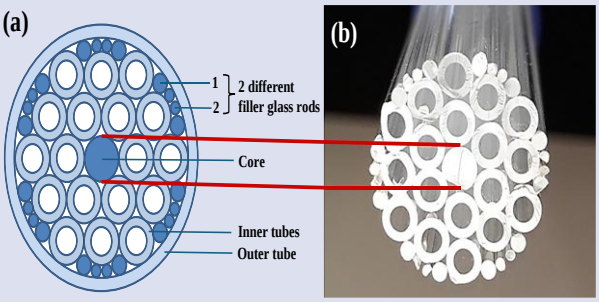

Figure 2. a. Design structure of LPF1 cross-section with one type of inner glass tube, 2 different filler rods, and a core rod placed in an outer tube, b. Image of LPF1 preform cross-section.

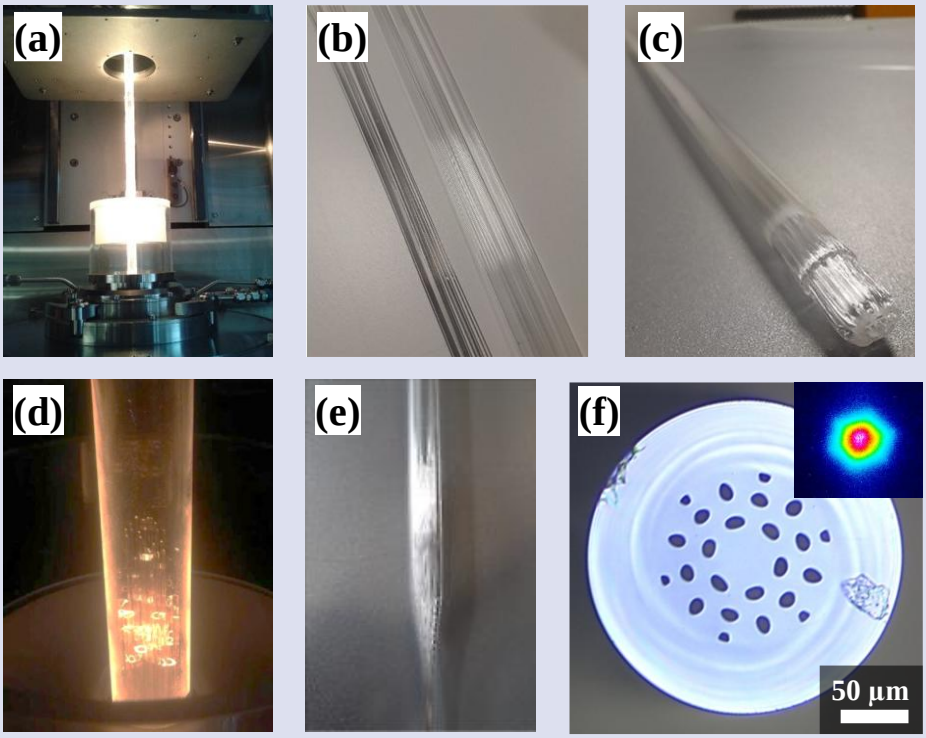

Figure 3. a. Pictures of fiber preform materials such as inner glass tubes, filler glass rods, and core drawing from in-house specialty fiber draw tower, b. the rods and tubes, c. assembled the fiber preform structure, d. and e. drawing of the fiber preform. f. microscope image of the passive LPF obtained from a single-step drawing process and the inset presents the near-field image of the output beam of the passive LPF.

LPF1 preform by using a well-known PCF fiber production method called the "stack-and-draw" procedure was fabricated initially. Figure 3 shows the production steps of an LPF fiber from the fabrication of LPF preform up to fiber. The preform sub-structures targeted in the design (inner tubes, core, and different size rods for fillers) were fabricated first by drawing glass tubes and rods from our high-temperature specialty fiber draw tower (see Figure 3a). In this work, the fused quartz rods and the tubing were purchased by Technical Glass Products, Inc. The index refraction of rquartz for all products is 1.4481 (@ 1200 nm). The quartz rods for the core region and the fillers were produced from the same glass initial rod under different drawing conditions. The inner tube size parameters regarding the inner and outer diameters were optimized by drawing carefully selected initial fused quartz tubing. The glass inner tubes and rods were manually assembled into a preform stack whose structure, as shown in Figure 3b, corresponds to the desired LPF structure. Figure 3c presents the assembled LPF preform structure. The total size of this preform can reach up to 16 mm in diameter.

This LPF preform was drawn to final LPF production using a single-step drawing process. Figure 3d shows an example of the drawn preform down to the final product. During the single-step drawing, the sub-structures (tubes and rods) of the LPF preform are fused to obtain a microstructured preform, which further leads to the final LPF production. The image of the fiber preform drawn is shown in Figure 3e. To optimize fiber structure and parameters such as the pitch, the diameters of the holes, the hole-diameter ratio, the core, and the outer diameter of the fiber, the effect of drawing process parameters were studied such as furnace temperature directly related to the preform temperature, preform feed speed, and drawing speed on the final product. The drawing speed of the LPF fiber was about 1 m/min. The result of the passive LPF obtained from a single-step drawing process is shown in Figure 3f. The cladding diameter of the produced LPF was measured to be 231 µm. From the fiber structure, the pitch (Λ) of 25.1 µm and the hole diameter of 11.4 µm can be deducted, which corresponds to the normalized hole diameter d/Λ of 0.454. The LPF structure core size could be estimated at 45.5 µm.

The beam localization and propagation into the core region of this LPF were also studied. To optimize the excitation of the fundamental mode (LP01 mode), the modal overlap with the Gaussian-shaped excitation infrared beam within the core area has been carefully performed. To observe the fundamental mode propagation into the fiber, the output beam from the end facet of the fiber onto a CCD camera was also checked. The inset of Figure 3f shows the emitted beam after propagation in a 1 m-long LPF. We didn't observe any leakage of the beam into the cladding region. The propagation loss of the LPF of ~ 1 dB/m was also measured. To prevent the effective single-mode operation of the LPF, the fundamental mode propagation was also disturbed by gently offsetting the coupling condition of the fiber and due to high losses on the HOMs, there is no HOMS propagation observed at the fiber end facet, which proves the evidence of the effective single-

mode operation of the LPF. The divergence and the beam quality of an emitted beam from the LPF are measured by using Thorlabs Complete M² Measurement Systems. The numerical aperture (NA) of the LPF of 0.044 and the M2 value of 1.2 were calculated. With these results, an effective single-mode operation has been performed from our first LPF design. But despite all these results, it has been noticed that the hole shape deformation of LPF has been affected due to the single-step drawing process and mainly missing filler rods between the inner tubes. To better control this issue, it has further developed our second LPF fiber preform design and applied the two-step drawing processing.

Fabrication of LPF with Two-step Drawing Processing

Figure 4a describes the detailed design of the LPF2 preform. In this design, a similar structure template was used shown in Figure 2a, but a thinner diameter of filler glass rods was added (24 pieces in total) to the areas between the inner tubes and the core shown in Figure 4a. To obtain a well-fused glass structure and a microstructured preform called “cane”, the drawing of the LPF2 preform has occurred from a 16 mm diameter of LPF2 preform to a 5 mm diameter of the LPF2 cane with a drawing speed of about 1 m/min. The cross-section image of the large-pitch fiber preform of the LPF2 after the first drawing is shown in Figure 4b. As a result of the first drawing on the LPF2 cane, it is seen that the structure of the LPF2 design is preserved without any deformation.

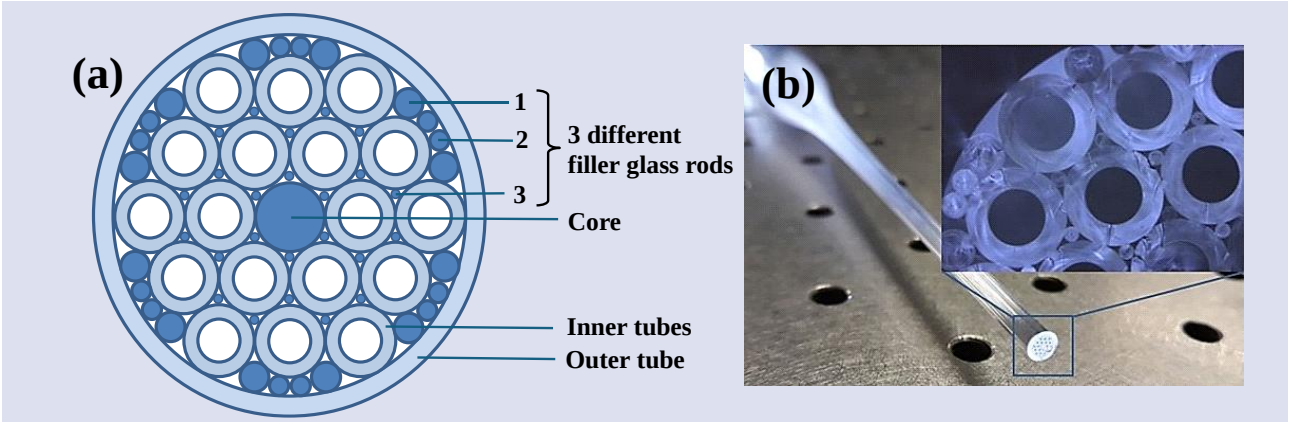

Figure 4. a. Design structure of LPF2 cross-section with one type of inner glass tube, 3 different filler rods, and a core rod placed in an outer tube, b. Image of the LPF2 preform cross-section after first drawing.

The second step in LPF fabrication involves drawing the LPF2 cane into an LPF2 with the desired dimensions and shape, such as pitch size, hole diameter, hole shape, and outer diameter of fiber. To study the effect of the normalized hole-diameter (d/Λ) parameters on the beam propagation behavior into the fiber, the drawing of the LPF2 cane has been performed with and without the air pressure applied inside the LPF2 cane. To eventually reduce the hole diameter value, the drawing of the LPF2 cane is first performed under a vacuum level of 10 mbar. The drawing speed of the LPF2 cane is about 3 m/min. The first fiber from the LPF2 cane is presented in Figure 5a. The pitch (Λ) of the fiber is about 29.2 µm, and the hole diameter is 5.7 µm, which corresponds to the normalized hole diameter d/Λ of 0.195. The LPF core size could be estimated at 55.3 µm. Then, the beam localization and propagation into this core region were studied. Even though it has been tried to excite the fundamental mode by changing the different modal overlaps (beam size, coupling angle, etc.) with the Gaussian-shaped excitation infrared beam within the core area, any fundamental mode propagation into the fiber has been observed at the end facet of the fiber onto a CCD camera. The near-field image of the output beam of the passive LPF with d/Λ ~ 0.195 obtained from a two-step drawing process is shown in Figure 5.

The leakage of the beam into the cladding region and the non-perfectly-localized beam into the core region has been observed.

In the next step, the drawing process of a similar LPF2 cane is then performed under no vacuum conditions with the top of the tube exposed to the ambient atmosphere. The drawing speed of the LPF2 cane is also performed at 3 m/min. The cross-section of fiber produced under these conditions is presented in Figure 5c. The larger hole diameter and smaller pitch size, compared to the fiber presented in Figure 5a, are obtained. From this fiber structure, the pitch (Λ) of 25.4 µm and the hole diameter of 8.2 µm have been deducted, which corresponds to the normalized hole diameter d/Λ of 0.322 with a relatively higher value compared to the fiber obtained in Figure 5a. This LPF core size could be estimated at 42.8 µm, and the cladding diameter of the produced LPF was measured to be 184 µm. Figure 5d presents the near-field image of the output beam of the passive LPF d/Λ ~ 0.322 obtained from a two-step drawing process using Thorlabs' complete M2 measurement system that includes the beam profiler in the near and far fields. The cross-section of beam-shaping 1 m-long LPF fiber at the end facet with a typical hexagonal mode field is obtained without any leakage of the beam into the cladding region. The propagation loss of this LPF of ~ 1 dB/m was also measured. The numerical aperture (NA) of this LPF of

0.044 and the M2 value of 1.2 were also calculated with similar parameters obtained in fiber produced and presented in Figure 3. With these results, an effective single-mode operation has also been performed from our second LPF design with the optimum drawing conditions. In addition, all fibers produced in the LPF2 approach demonstrate a circular hole-shaped structure compared to the approach presented in the LPF1 production.

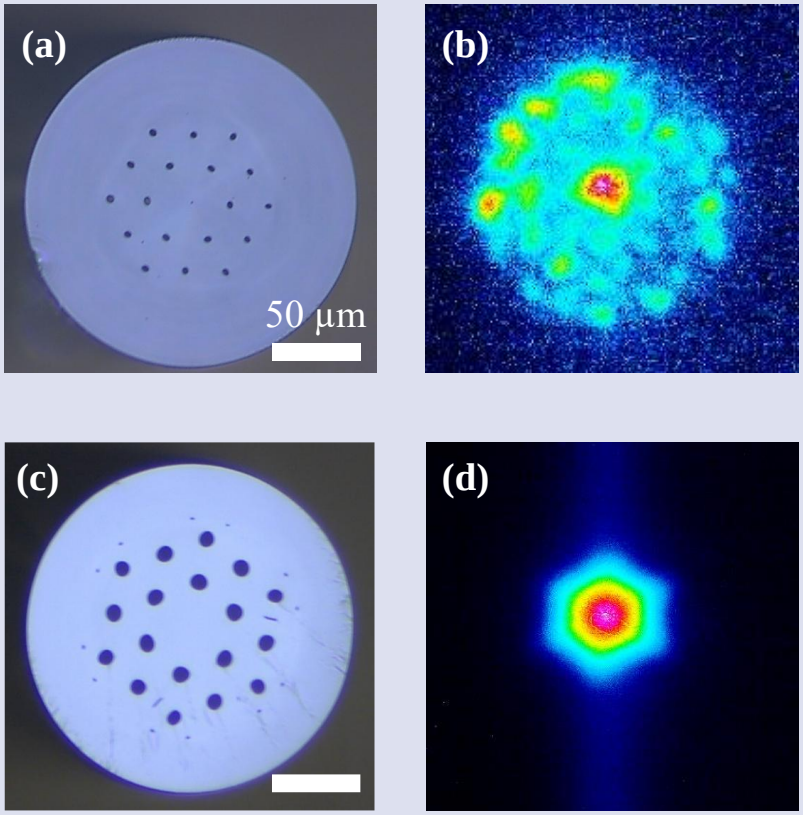

Figure 5. Microscope and near-field images of the output beam of the passive LPFs with d/Λ ~ 0.195 (a, b) and d/Λ ~ 0.322 (c, d) obtained from a two-step drawing process.

Numerical Simulation of LPF

To investigate the guiding properties of our optical fiber, the finite element method based on COMSOL Multiphysics software 5.0 is performed to simulate the proposed LPF2 with d/Λ ~ 0.322. The structural parameters of LPF2 utilized in the simulations are shown in Table 1.

Table 1. The Simulation parameters of the LPF with 2 air rings conducted using the FEM in COMSOL Multiphysics.

Parameters	Value
Air Hole diameter	8.2 µm
Pitch distance	25.4 µm
Normalized hole diameter	0.322
The Refractive index of air	1.0
The refractive index of the cladding	1.4481 (@ 1200 nm)
Number of air rings	2

Modeling the LPF can be more challenging than typical single-mode fibers due to the variation in the estimation of the effective refractive index of the fundamental mode that depends on the LPF parameters and operational wavelength [20]. When the air hole diameter to pitch distance ratio (d/Λ) is around 0.3 and the operational wavelength (λ) is between 0.8 µm and 1.6 µm, the effective refractive index of the fundamental mode must be searched around 1.447 and 1.449. Figure 6 shows the design of the LPF with d/Λ ~ 0.322 and the fundamental mode electric field distribution where the mode field diameter can reach up to 72 µm. On the other hand, the loss due to waveguide geometry in the LPF is calculated using the confinement loss, which is determined using the equation [16, 22]:

$$L_c = -20\log_{10}\ \varepsilon^{-kIm[n_{eff}]} = 8.686kIm[n_{eff}] \qquad (1)$$

Where $\varepsilon^{-kIm[n_{eff}]}$ *the term* suggests an exponential decay, k is the propagation constant in free space that equals to $2\pi/\lambda$ and Im(neff) is the imaginary part of the refractive index

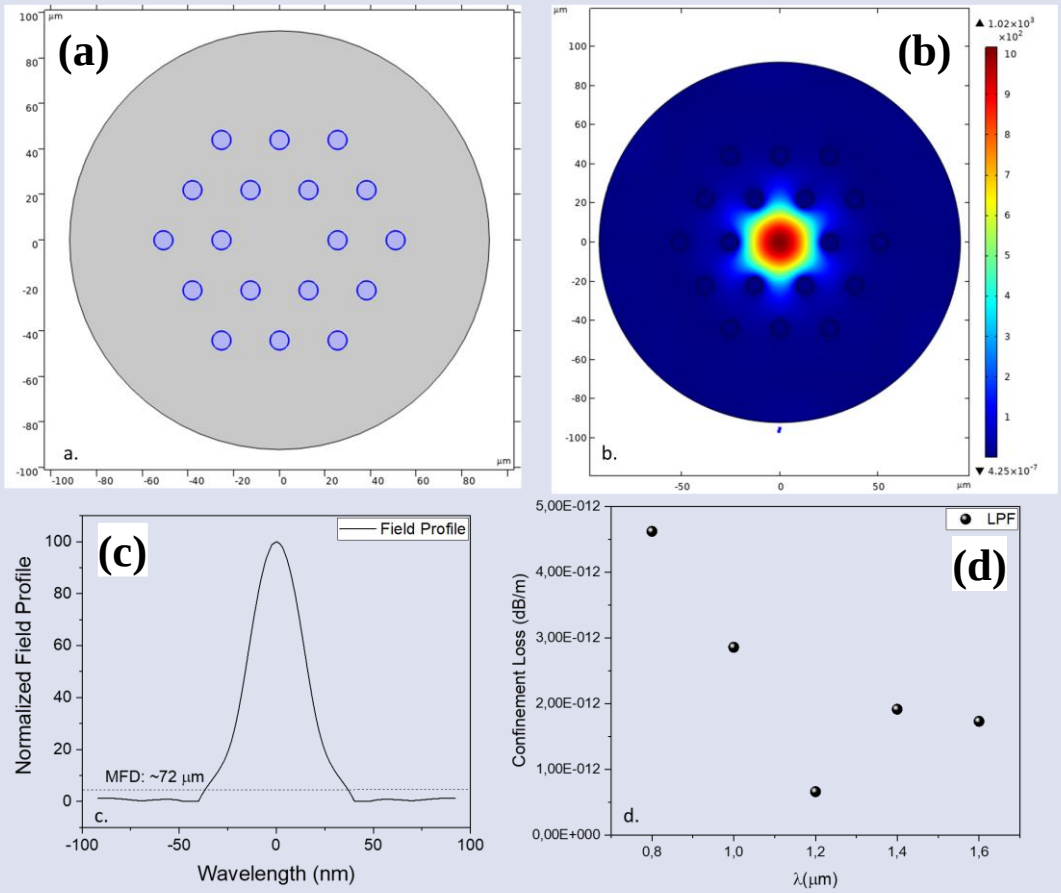

Figure 6. a. Geometry of the designed large pitch photonic crystal fiber (LPF) when d/Λ ~ 0.322, b. fundamental mode at the wavelength of 1200 nm, c. the field line profile of the fundamental mode along LPF center and d. the confinement loss in dB/m between 800 nm and 1600 nm.

The lowest confinement loss of the LPF with d/Λ ~ 0.322 is at the wavelength of 1.2 µm with a loss value of 6.5934×10-13 dB/m. This value is consistent with the previous LPF studies where the confinement loss was reported [23]. Such low-loss design of the LPF gives valuable insights, and the numerical simulation demonstrates that the light propagation behaviors of our fiber produced from LPF2 preform agree well with the experiment results.

Conclusions

Two different fabrication processes for the single transverse mode passive LPFs were described. In the first approach, the preform design of LPF with one type of inner glass tube, 2 different filler rods, and a core rod placed in an outer tube was produced by using the draw-and-stack technique. The passive LPF was obtained from a single-step preform drawing process. The single transverse mode propagation from this LPF, which has a core size of 45.5 µm and a normalized hole diameter of 0.454, is observed. The missing filler rods between the inner tubes and direct size reduction from the preform with a mm diameter down to fiber with a diameter of around ~ 200 µm results in the hole shape deformation from the circular hole shape of the initial inner tubes to the elliptical-like hole-shape in the LPF. In the second approach, the areas between the inner tubes and the core were filled by using the additional filler rods, and a two-step drawing process was performed. This second approach allowed for the control conditions of the fiber structure. The LPF with the circular hole shape was successfully produced. The single transverse mode propagation from this LPF, which has a core size of 42.8 µm and a normalized hole diameter of 0.322, is also demonstrated. In other words, the one-step drawing condition and the two-step conditions do not give the same quality fibers since the latter, where two-step drawing conditions are applied, provides more control in the size and the shape of the air holes. Therefore, the second method yields the PCF satisfying the single-mode criteria. The fundamental mode propagation into the core region was also numerically confirmed for an LPF having a normalized hole-diameter (d/Λ) value around 0.322. These results also reinforced our understanding of how such structural parameters influence mode behavior within the LPF. This development aligns with our findings, as it also resulted in more freedom to control the fiber structure, enhancing the potential applications significantly. Future studies can focus on the fabrication of such fiber structures with double-clad active fiber concepts for further fiber lasers and amplifier systems.

Conflict of interests

There are no conflicts of interest in this work.

Acknowledgments

This work was partially supported by the Scientific and Technological Research Council of Turkey (TÜBİTAK) (Project No: 113A055). Dr. Bülend Ortaç gratefully acknowledges support from TÜBİTAK, the Turkish Academy of Sciences Outstanding Young Scientists (TÜBA-GEBİP), the Young Scientist Awards Program (BAGEP) from the Science Academy, as well as the METU Prof. Dr. Mustafa Parlar Foundation Research Incentive and Feyzi Akkaya Foundation (FABED) Eser Tümen Young Scientist Awards programs. The author acknowledges the infrastructural support provided by the National Nanotechnology Research Center (UNAM) at Bilkent University. Appreciation is also extended to Dr. Ali Karatutlu, Dr. Esra Kendir Tekgül, Elif Yapar Yıldırım, Ekin Teslime Balk, Ahmet Başaran, and Ahmet Kağan Kolsuz for their fruitful discussions and infrastructural support. Additionally, the author recognizes Seyitali Yaşar and Levent Ersoy at Bilkent University-UNAM for their technical assistance during the drawing process.

References

[1] Jauregui, C., Limpert, J., Tünnermann, A., High-power fibre lasers, *Nature Photonics.* 7 (2013) 861-867.

[2] Zervas, M., Codemard, C., High Power Fiber Lasers: A Review, *IEEE J. SEL. TOP. QUANT.* 20 (2014) 1-23.

[3] Zuo, J., Lin, X., High-Power Laser Systems, *Laser Photonics Rev.* 16 (5) (2022) 826-831.

[4] Chen, X., Yao, T., Huang, L., An, Y., Hanshuo, W., Pan, Z., Zhou, P., Functional Fibers and Functional Fiber-Based Components for High-Power Lasers, *Advanced Fiber Materials*, 5 (2023) 59-106.

[5] Taverner, D., Richardson, D. J., Dong, L., Caplen, J., 158 μJ pulses from a single-transverse-mode, large-mode-area erbium-doped fiber amplifier, *Optics Letters*, 22 (6) (1997) 378-380.

[6] Broderick, N., Offerhaus, H., Richardson, D. J., Sammut, R. A., Caplen, J., Dong, L., Large Mode Area Fibers for High Power Application, *Optical Fiber Technology*, 5 (1999) 185-196.

[7] Jauregui, C., Stihler, C., Limpert, J., Transverse mode instability, *Advances in Optics and Photonics*, 12 (2020) 429-484.

[8] Xiuquan, M., Cheng Z., I-Ning H., Alex K., Almantas G., Single-mode chirally-coupled-core fibers with larger than 50 μm diameter cores, *Optics Express*, 22 (2014) 9206-9219.

[9] Marko L., Mette M. J., Kristian R. H., Thomas T. A., Jes B., Jesper L., Distributed mode filtering rod fiber amplifier delivering 292W with improved mode stability, *Optics Express*, 20 (2012) 5742-5753.

[10] Liang D., Hugh A. M., Libin F., Michiharu O., Andrius M., Shigeru S., Martin E. F., Ytterbium-doped all glass leakage channel fibers with highly fluorine-doped silica pump cladding, Optics Express, 17 (2009) 8962-8969.

[11] Wang, X., Lou, S., Lu, W., Sheng, X., Zhao, T., Hua, P., Bend resistant large mode area fiber with multi-trench in the core, IEEE J. SEL. TOP. QUANT. 22 (2016).

[12] Gu, G., Kong, F., Hawkins, T. W., Jones, M., Dong, L., Ytterbium-doped all glass leakage channel fibers with highly fluorine-doped silica pump cladding, *Optics Express*, 23 (2015) 9147-9156.

[13] Yehouessi, J. P., Vanvincq, O., Cassez, A., Douay, M., Quiquempois, Y., Bouwmans, G., Bigot, L., Extreme large mode area in single-mode pixelated Bragg fiber, *Optics Express*, 24 (2016) 4761-4770.

[14] Limpert, J., Stutzki, F., Jansen, F., Otto, H.-J. Eidam, T. Jauregui, C., Tünnermann, A., Yb-doped large-pitch fibres: Effective single-mode operation based on higher-order mode delocalisation, *Light: Science & Applications,* 1 (2012) e8.

[15] Stutzki, F., Jansen, F., Otto H.-J., Jauregui, C., Limpert, J., Tünnermann, A., Designing advanced very-large-mode-area fibers for power scaling of fiber-laser systems, *Optica*, 1 (2014) 233-242.

[16] Steinkopff, A., Jauregui, C., Stutzki, F., Nold, J., Hupel, C., Haarlammert, N., Bierlich, J., Tünnermann, A., Limpert, J., Transverse single-mode operation in a passive large pitch fiber with more than 200 μm mode-field diameter, *Optics Letters*, 44 (2019) 650-653.

[17] Stutzki, F., Jansen, F., Eidam, T., Steinmetz, A., Jauregui, C., Limpert, J., Tünnermann, A., High average power large-pitch fiber amplifier with robust single-mode operation, *Optics Letters*, 36 (2011) 689-691.

[18] Martin, B., Florian, J., Fabian S., Cesar J., Ortaç, B., Limpert, J., Tünnermann, A., High average and peak power femtosecond large-pitch photonic-crystal-fiber laser," *Optics Letters*, 36 (2011) 244-246.

[19] Stark, H., Buldt, J., Mueller, M., Klenke, A., Tünnermann, A., Limpert, J., 23 mJ high-power fiber CPA system using electro-optically controlled divided-pulse amplification, *Optics Letters*, 44 (2019) 5529-5532.

[20] Mortensen, N.A., Folkenberg, J.R., Nielsen, M.D., Hansen, K.P., Modal cutoff and the V parameter in photonic crystal fibers, *Optics Letters,* 28 (2003), 1879-1881.

[21] Suslov, D., Komanec, M., Nemecek, T., Bohata, J., Zvanovec, S., Exact modeling of photonic crystal fibers for determination of fundamental properties, *Optical Fiber Technology*, 56. (2020) 102177.

[22] Träger, F., Handbook of Lasers and Optics. Springer, (2012).

[23] Pandey, S., Prajapati, Y., Maurya, J., Design of simple circular photonic crystal fiber having high negative dispersion and ultra-low confinement loss, *Results in Optics*, 1 (2020).